ELSEVIER

Nuclear Instruments and Methods in Physics Research B 191 (2002) 437–441

NIM B
Beam Interactions with Materials & Atoms

www.elsevier.com/locate/nimb

Ferromagnetic FePt nanoparticles formed in Al_2O_3 by ion implantation

C.W. White [a,*], S.P. Withrow [a], J.D. Budai [a], L.A. Boatner [a], K.D. Sorge [b], J.R. Thompson [b], K.S. Beaty [c], A. Meldrum [c]

[a] *Oak Ridge National Laboratory, P.O. Box 2008, Oak Ridge, TN 37831-6057, USA*
[b] *University of Tennessee, Knoxville, TN 37996, USA*
[c] *University of Alberta, Edmonton AB T6G 2J1, Canada*

Abstract

Oriented, ferromagnetic FePt nanoparticles have been produced in Al_2O_3 single crystals by ion implantation and annealing. FePt orientation and particle size depends strongly on the implantation conditions. Magnetic coercivities of these nanocomposites are extremely high, reaching values in excess of 20 kOe for Pt concentrations of ~45% in the FePt alloy. The formation of ferromagnetic FePt nanoparticles in fused SiO_2 is also demonstrated. © 2002 Elsevier Science B.V. All rights reserved.

Keywords: FePt nanoparticles; Ferromagnetic nanoparticles; Oriented nanoparticles; Ordered alloy

1. Introduction

The growth and microstructure of FePt films or nanoparticles are of significant interest since this alloy can form the chemically ordered, tetragonal $L1_0$ phase that exhibits an extremely high magnetic anisotropy. Materials with this property are attractive candidates for ultrahigh density magnetic data recording [1]. Films of $Fe_{1-x}Pt_x$ (with $x \sim 0.5$), with a high magnetic anisotropy have previously been prepared by techniques such as MBE [2], cosputtering [3], or by the subsequent ion irradiation of films deposited at low temperature [4]. FePt nanoparticles have also been synthesized chemically as an ordered superlattice of particles [5] and FePt nanoparticles have been encapsulated in amorphous SiO_2 [6] or Al_2O_3 [7,8].

In this work, we have used the sequential ion implantation of Fe and Pt followed by thermal annealing to form $Fe_{1-x}Pt_x$ nanoparticles that are embedded in Al_2O_3 single crystals. The nanoparticles are oriented with respect to the matrix and the orientation and microstructure depend strongly on the implantation parameters. The chemically ordered, tetragonal $L1_0$ structure is formed over a wide range of Pt concentrations. The FePt nanoparticles are ferromagnetic and the magnetic coercive field is very high, reaching a maximum value at a Pt atomic fraction of ~45% with a coercive field that exceeds 20 kOe. Ion implantation followed by thermal annealing should find applications in the formation of ferromagnetic FePt nanoparticles that are encapsulated in a variety of

* Corresponding author. Tel.: +1-865-574-6295; fax: +1-865-576-8135.
E-mail address: whitecw@ornl.gov (C.W. White).

0168-583X/02/$ - see front matter © 2002 Elsevier Science B.V. All rights reserved.
PII: S0168-583X(02)00588-8

other matrices. The formation of FePt precipitates by ion implantation and annealing is also reported here for the case of an amorphous, SiO_2 matrix.

2. Experimental procedure

For the formation of FePt nanoparticles in Al_2O_3, *c*-axis-oriented single crystals of Al_2O_3 were used as substrates. Energies for the Fe ions (350 keV) and Pt ions (910 keV) were chosen to give an overlap of the concentration profiles with projected ranges of ~175 nm. An implant dose of $1 \times 10^{17}/cm^2$ for Fe was used in each case and the Pt dose was chosen to give the desired Pt atomic fraction x (where $x = Pt/(Fe + Pt)$) in the alloy. Samples were prepared with x in the range of 25–55%. Samples were implanted at either high temperature (550 °C for Fe, 500 °C for Pt) or at a somewhat lower temperature (200 °C for both Fe and Pt). Elevated temperature implantation was utilized to try to maintain crystallinity in the Al_2O_3 matrix during implantation. Following implantation, the samples were annealed for 2 h at 1100 °C in flowing Ar + 4% H_2, followed by slow cooling to room temperature. The samples were characterized by Rutherford backscattering (RBS) ion channeling (2.3 MeV He), by X-ray diffraction (Cu K_α radiation using both four circle and powder diffractometers) and by transmission electron microscopy (TEM). The magnetic properties were measured using a SQUID magnetometer at temperatures of 5–400 K in applied fields up to 65 kOe. For the data presented here, the diamagnetic background of the Al_2O_3 host was subtracted.

3. Results

Fig. 1 shows the X-ray diffraction and TEM results for one of the Pt-rich alloy samples ($Fe_{48}Pt_{52}$) The $\theta - 2\theta$ scan along the *c*-axis of Al_2O_3 shows the strong (0 0 6) diffraction line expected for Al_2O_3. The other diffraction lines in Fig. 1(a) arise from the face centered tetragonal (fct) phase of FePt. This phase exhibits the $L1_0$ structure that consists of alternating planes of Fe and Pt atoms stacked along the ⟨0 0 1⟩ axis of the alloy. The X-ray results show that the FePt nanoparticles are oriented along the Al_2O_3 host *c*-axis, but that there are multiple orientations of the FePt nanoparticles (i.e. FePt (0 0 1), (1 1 0), (1 1 1) and several other orientations). In Fig. 1(a), there are four superlattice reflections (denoted by s) as well as several fundamental reflections from fct FePt. The existence of the superlattice reflections demonstrates that at least some of the nanoparticles are chemically ordered with the $L1_0$ structure. The order parameter is a measure of the degree of ordering and a rough estimate can be obtained by

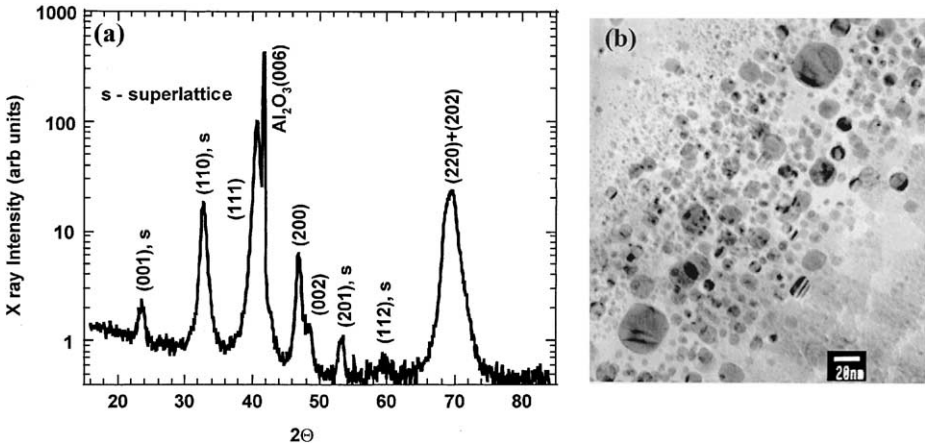

Fig. 1. X-ray diffraction (a) and cross-section TEM (b) results for *c*-axis. Al_2O_3 crystals implanted by Fe (350 keV, $1 \times 10^{17}/cm^2$, 550 °C) + Pt (910 keV, $1.1 \times 10^{17}/cm^2$, 500 °C) followed by annealing (1100 °C/2 h/Ar + 4% H_2).

comparing the integrated intensities of the superlattice and corresponding fundamental reflections. For the results in Fig. 1, the order parameter approaches unity for the (0 0 1) and (1 1 0) oriented nanoparticles, showing that, in these nanoparticles, almost all of the atoms occupy the proper lattice positions. Therefore, the ordered alloy is being formed as a result of ion implantation and annealing. Fig. 1(b) is a cross-section TEM micrograph showing the microstructure in the vicinity of the peak concentration in the Fe and Pt profiles. FePt nanoparticles are clearly observed in the micrograph and most are in the size range of 2–10 nm in diameter, with a few FePt precipitates as large as ~25 nm.

Fig. 2 illustrates the magnetic properties for FePt nanoparticles formed by high-temperature ion implantation (550 °C Fe/500 °C Pt). Fig. 2(a) shows the magnetization curves (measured at 5 K) for a sample with the alloy composition $Fe_{55}Pt_{45}$. Magnetization curves are shown for the applied field oriented perpendicular and parallel to the Al_2O_3 host crystal surface. For both field orientations, the magnetization curves may not be completely saturated even at applied fields as large as 65 kOe. The coercive field (H_c) deduced from these results was ~22 kOe, but this is a lower limit to the true coercive field since the magnetization may not be saturated. This coercive field value is much greater than that measured for Al_2O_3 implanted by Fe alone (~140 Oe at 5 K). The coercive field for the $Fe_{55}Pt_{45}$ sample remains in excess of 18 kOe even at temperatures as high as 300 K. These values of the coercive field are considerably greater than those reported previously [5–8] for FePt nanoparticles. The coercive fields deduced from the two applied magnetic field orientations are nearly the same, which is not unexpected since very few of the nanoparticles are oriented with their easy axis of magnetization (⟨0 0 1⟩) normal to the surface. For both orientations, there is a pronounced shoulder near H=O in the magnetization curves. An appropriate explanation for this shoulder will require further research, but it may be related to the existence of larger FePt particles with multidomain states, as suggested by others [9].

Fig. 2(b) shows the H_c coercive field values deduced for samples with different Pt atomic fractions x. Coercive field is a strong function of the FePt alloy composition and it reaches a maximum of ~22 kOe at $x \sim 45\%$. This dependence H_c on x is in good agreement with the results obtained by others using the chemical synthesis of FePt nanoparticles with different Pt concentrations [8], but the coercive fields of the samples in Fig. 2(a) are considerably higher than those reported in [8]. For the sample with a Pt concentration of ~25%, the coercive field is nearly zero, even at 5 K. X-ray diffraction measurements for this sample are consistent with the cubic $L1_2$ structure expected for Fe_3Pt. Measured diffraction patterns for the other

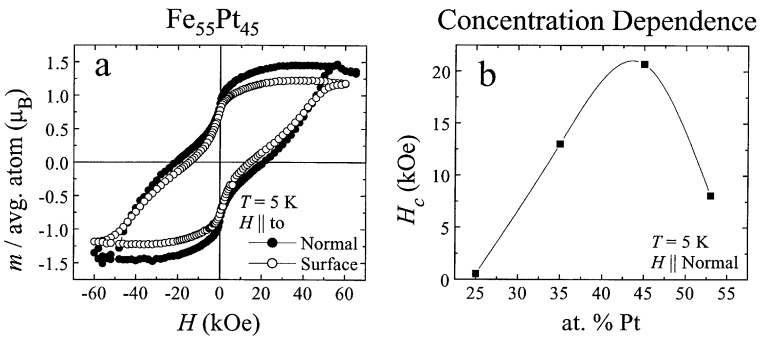

Fig. 2. Magnetic properties of $Fe_{1-x}Pt_x$ nanoparticles in Al_2O_3. Magnetization curves for $Fe_{55}Pt_{45}$ are shown in 2(a). The dependence of the coercive field H_c on Pt atomic fraction is shown in Fig. 2(b). Coercive fields were measured for the applied field perpendicular to the sample surface except for the sample with the lowest concentration.

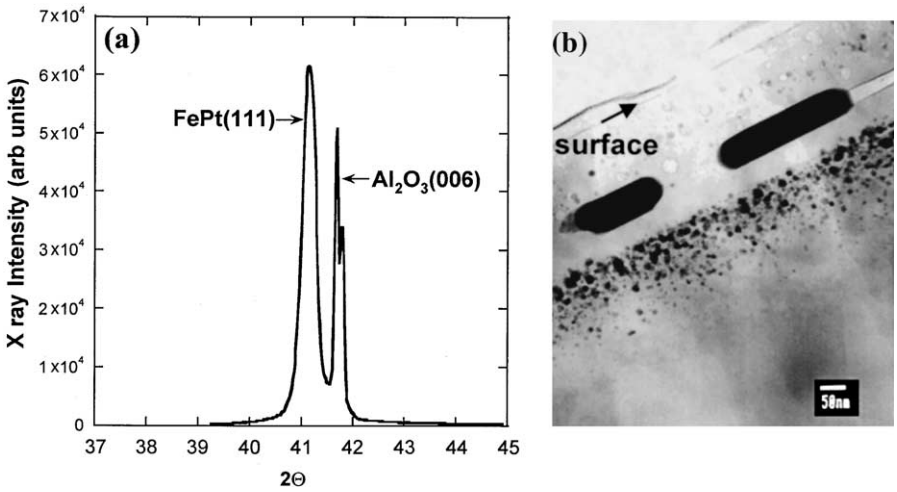

Fig. 3. X-ray diffraction (a) and cross-section TEM (b) results for $Fe_{55}Pt_{45}$ nanoparticles formed in Al_2O_3 by implantation at 200 °C followed by annealing (1100 °C/2 h/Ar + 4% H_2).

samples of Fig. 2(b) are consistent with those expected for the fct $L1_0$ structure of $Fe_{1-x}Pt_x$ and it is these samples that exhibit the very high H_c values.

If the implantation temperature is reduced to 200 °C for both Fe and Pt, then very large nanoparticles with a single orientation can be produced as shown by the results presented in Fig. 3. In the diffraction spectra, the only alloy line observed is the intense FePt (1 1 1) reflection showing that almost all of the nanoparticles have their ⟨1 1 1⟩ axis parallel to the *c*-axis of Al_2O_3. The FePt particle size (Fig. 3(b)) is much larger than that corresponding to Fig. 1(b). Particle sizes of more than 200 nm are observed in TEM cross-section views. In plan view (not shown), the FePt particles exhibit a threading, worm-like particle shape that can extend for more than 1 μm. The magnetic properties in this case are comparable with those obtained by implanting Fe and Pt at higher temperatures. Consequently, by implanting at temperatures of 200 °C followed by annealing, the $Fe_{55}Pt_{45}$ particles are relatively large and they exhibit a single orientation where the (1 1 1) FePt is parallel to the Al_2O_3 *c*-plane. RBS channeling measures suggest that a buried amorphous layer is formed in Al_2O_3 by implantation at a temperature of 200 °C. Following annealing, the ion channeling in the Al_2O_3 matrix is good suggesting that crystallization of the amorphous layer has occurred from both interfaces during annealing accompanied by segregation of the Fe and Pt into a semi-continuous layer thus forming large particles. The formation of the buried amorphous phase can be avoided at these doses by implanting at higher temperatures, but the resulting FePt nanoparticles are significantly smaller and they exhibit multiple crystallographic orientations relative to the *c*-axis of the Al_2O_3 host (Fig. 1).

Ferromagnetic FePt nanoparticles can also be produced by ion implantation and annealing in other matrices. One example is shown by the TEM results of Fig. 4 for Fe and Pt implanted into fused SiO_2 at elevated temperatures and subsequently annealed. A band of $Fe_{55}Pt_{45}$ particles, some as large as 75 nm, is located near the peak of the implant concentration profile. X-ray diffraction results show the nanoparticles to be randomly oriented but in the chemically ordered $L1_0$ phase of FePt. Magnetization curves for this nanocomposite are shown in Fig. 5. The coercive field deduced from the measurement is extremely high (almost 30 kOe) and this is considerably greater than that resulting from the annealing of deposited $FePt/SiO_2$ multilayers (~15 kOe) [6]. The coercive field is a strong function of the Pt concentration in the alloy and the detailed results for the $FePt/SiO_2$ system will be reported separately.

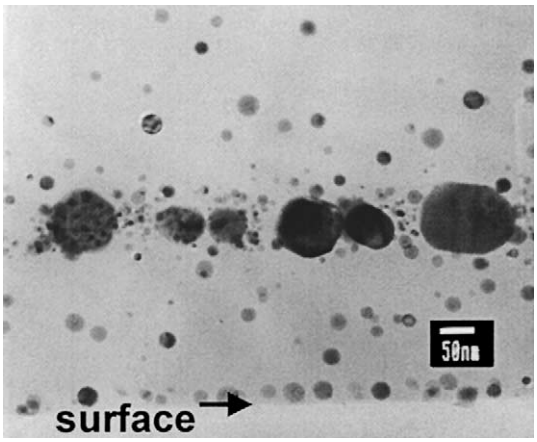

Fig. 4. Cross-section TEM results showing the $Fe_{55}Pt_{45}$ nanoparticles formed in SiO_2 implanted by Fe (350 keV, $1 \times 10^{17}/cm^2$, 550 °C) + Pt (910 keV, $8.2 \times 10^{16}/cm^2$, 500 °C) followed by annealing (1000 °C/2 h/Ar + 4% H_2).

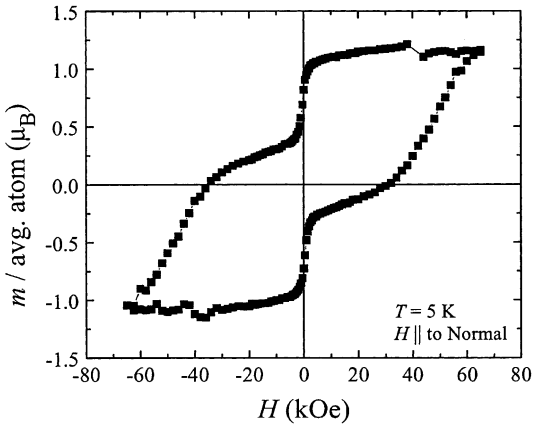

Fig. 5. Magnetization measurements for the sample of Fig. 4.

4. Conclusions

Ferromagnetic $Fe_{1-x}Pt_x$ nanoparticles with extremely high coercivities have been produced in Al_2O_3 single crystals by implantation. Implantation at elevated temperatures (~500 °C) followed by annealing gives rise to small nanoparticles (up to ~25 nm) that exhibit multiple orientations, whereas implantation at ~200 °C for the same dose gives rise to a buried layer of very large FePt particles oriented with the ⟨1 1 1⟩ FePt direction parallel to the Al_2O_3 *c*-axis. In both cases, the magnetic coercive fields are found to be extremely high (>20 kOe) at 5 K and they remain in excess of 18 kOe at room temperature. Ferromagnetic FePt nanoparticles can also be formed in amorphous SiO_2. A coercive field of almost 30 kOe has been measured for $Fe_{55}Pt_{45}$ nanoparticles formed in SiO_2 by implantation at elevated temperatures followed by annealing. The maximum FePt nanoparticle size in this case is ~75 nm.

Acknowledgements

Oak Ridge National Laboratory, managed by UT-Battelle, LLC, for the US Dept. of Energy under contract DE-AC05-00OR22725.

References

[1] D. Weller, A. Moser, L. Folks, M.E. Best, W. Lee, M.F. Toney, M. Schwickert, J.-U. Thiele, M.F. Doerner, IEEE Transactions on Magnetics 36 (2000) 10.
[2] R.F.C. Farrow, D. Weller, R.F. Marks, M.F. Toney, D.J. Smith, M.R. McCartney, J. Appl. Phys. 84 (1998) 934.
[3] M.R. Visokay, R. Sinclair, App. Phys. Lett. 66 (1995) 1692.
[4] D. Ravelosona, C. Chappert, V. Mathet, H. Bernas, Appl. Phys. Lett. 76 (2000) 236.
[5] S. Sun, C.B. Murray, D. Weller, L. Folks, A. Moser, Science 287 (2000) 1989.
[6] C.P. Luo, D.J. Sellmyer, Appl. Phys. Lett. 75 (1999) 3162.
[7] M. Watanabe, T. Masumoto, D.H. Ping, K. Hono, Appl. Phys. Lett. 76 (2000) 3971.
[8] B. Bian, D. Laughlin, K. Sato, Y. Hirotsu, J. Appl. Phys. 87 (2001) 6962.
[9] I. Panagiotopoulos, S. Stavroyiannis, D. Niarchos, J.A. Christodoulides, G.C. Hadjipanayis, J. Appl. Phys. 87 (2000) 4358.